Lignin and Starch Derivatives with Selenium Nanoparticles for the Efficient Reduction of Dyes and as Polymer Fillers

Anna Modrzejewska-Sikorska [1],*[ID], Mariola Robakowska [2],*[ID], Emilia Konował [1][ID], Hubert Gojzewski [3], Łukasz Gierz [4],*[ID], Bartosz Wieczorek [4], Łukasz Warguła [4][ID] and Wiktor Łykowski [4]

[1] Faculty of Chemical Technology, Institute of Chemistry and Technical Electrochemistry, Poznan University of Technology, Berdychowo 4, 60-965 Poznan, Poland; emilia.konowal@put.poznan.pl
[2] Faculty of Chemical Technology, Institute of Chemical Technology and Engineering, Poznan University of Technology, Berdychowo 4, 60-965 Poznan, Poland
[3] Sustainable Polymer Chemistry, Department of Molecules & Materials, Faculty of Science and Technology, University of Twente, 7522 NB Enschede, The Netherlands; h.gojzewski@utwente.nl
[4] Faculty of Mechanical Engineering, Institute of Machine Design, Poznan University of Technology, Piotrowo 3, 60-965 Poznan, Poland; bartosz.wieczorek@put.poznan.pl (B.W.); lukasz.wargula@put.poznan.pl (Ł.W.); wiktor_lykowski@o2.pl (W.Ł.)
* Correspondence: anna.modrzejewska-sikorska@put.poznan.pl (A.M.-S.); mariola.robakowska@put.poznan.pl (M.R.); lukasz.gierz@put.poznan.pl (Ł.G.); Tel.: +48-61-6652311 (A.M.-S.); +48-61-6653683 (M.R.); +48-61-2244516 (Ł.G.)

Abstract: Selenium nanoparticles (SeNPs) were synthesized and stabilized by biopolymers, namely, sodium lignosulfonate (LS) and starch sodium octenyl succinate (OSA). The obtained selenium nanoparticles were studied for their catalytic activity in the reduction of a dye (C.I. Basic Blue 9, methylene blue) by sodium borohydride. The SeNPs-OSA and SeNPs-LS nanoparticles were also dispersed in a photosensitive matrix and studied as polymer composites. The research confirmed the catalytic abilities of the prepared SeNPs in the reduction of the organic dye. Mechanical tests on the polymers and their composites showed an improvement in the composites' strength in all tested cases. An increase in hardness and Young's modulus values of the filled materials compared to the pure matrix was found as well.

Keywords: selenium nanoparticles; lignosulfonate; starch sodium octenyl succinate; biopolymer; organic dye

1. Introduction

Selenium nanostructures (SeNPs) are particles of elemental selenium or its aggregates with the size in the order of nanometers. SeNPs can take a spherical form, but also appear as nano-ribbons or nano-rods [1,2]. SeNPs find a wide range of applications in many fields of science, industry, and technology. They unveil, similar as other nanoparticles, interesting chemical and physical properties and characteristics, i.e., catalytic, thermoelectric, optical, and piezoelectric properties, as well as very good photoconductivity [3–7]. For this reason, they are used in electronics and xerography, in the utility glass industry, biomedicine, pharmacy, as well as biotechnology and, due to their high antioxidant capacity, in the packaging industry, as additives to materials whose main component is plastics.

The desired properties of SeNPs, such as size, shape, and surface charge, are driven by the choice of the processing routes—physical, chemical, and biological [8–12]. The physical routes can employ, for instance, solvothermal synthesis, microwave treatment, electrodeposition, or pulsed laser ablation using an excimer laser [8,9]. The chemical routes can employ reduction, i.e., reducing selenium salts to stable colloidal suspensions. This reduction is most often carried out with the participation of surfactants or ascorbic acid [11]. This method requires the appropriate selection of a stabilizer, a reducing agent, and a solvent. However, some chemical reactions accompanying the production of selenium

nanostructures may adversely affect the environment. The biological route usually involves an alternative processing, which includes biological and green synthesis; both are simple and cheap and lack a negative environmental impact. The biological synthesis uses bacteria that reduce a selenium ion to a nanoparticle, while the green synthesis uses metabolites from plant extracts that can act as potential selenium-reducing agents. In addition, fungi can also be used in the production of SeNPs [2,10–12].

Lignin and starch are crucial renewable feedstocks. Especially, lignin is seen as a candidate for replacing non-biodegradable fossil-derived plastics, as it is the second abundant biopolymer in the world [13,14]. The use of lignin or starch derivates, such as sodium lignosulfonate and starch octenyl succinate, in the preparation of SeNPs can require a specific combination of a chemical method and green chemistry. Both types of these bio-based compounds can act as stabilizers for the selenium nanostructures produced [15,16]. The use of sodium lignosulfonate as a stabilizer allows obtaining SeNPs in liquid form, while the use of a starch octenyl succinate results in selenium nanostructures on a solid matrix.

Lignosulfonates (LSs) are anionic polyelectrolytes containing a significant number of sulfonic groups. They are produced in a large amount—approx. 1 million tons of dry matter per year worldwide [17]. The structural and chemical properties of lignosulfonates include their relatively high molecular weight (15,000–50,000 g/mol), solubility in water, a high degree of polydispersity, and a high ash content [18]. Due to the presence of hydrophobic chains and numerous hydrophilic functional groups in their structure, in aqueous solutions they have surface-active properties [19]. Many potential industrial applications [20,21] are linked to the presence of a multitude of functional groups such as carboxyl, phenolic, and sulfonic groups in the structure of LSs [22–24]. According to the literature, this is the reason why LSs have already been used, among others, as reducers and stabilizers in the manufacturing of gold and silver nanostructures [25–27]. Water-soluble lignosulfonates (LSs) were used for a simple and inexpensive synthesis of gold [25], while silver [26] nanoparticles in aqueous solutions at room temperature during the reaction with gold or silver salts. As a possible application, the obtained nanoparticles were studied for their catalytic activity in the reduction of organic dyes by sodium borohydride [26].

Starch $(C_6H_{10}O_5)_n$ is a glucose polymer, specifically, a biopolymers of a plant origin. Due to the presence of free hydroxyl groups in its structure, it can be relatively easily modified. One of the modified starches is sodium starch octenyl succinate (OSA). The synthesis of OSA starch was patented by Caldwell and Wurzburg [28,29]. The synthesis requires a cyclic octenyl succinic acid anhydride and starch under basic conditions. The obtained starch derivate has favorable emulsifying and stabilizing properties due to the presence of both hydrophobic and hydrophilic groups on its surface.

Synthetic dye pollutants in water are hazardous for plants, animals, and humans and cause environmental problems [30]. The removal of the synthetic dye contaminants pose both scientific and industrial challenges [31]. However, it was suggested that SeNPs are among the most promising agents for their efficient catalytic activity in degrading hazardous dyes such as methylene blue and bromothymol blue and others organic compounds in water. SeNPs are also attracting increasing attention due to their low toxicity, as well as their potential use in disease prevention and treatment [32].

Using SeNPs as fillers in polymer (nano)composites to fine-tune the characteristics of polymer matrices is of interest as well [33,34]. Different polymer composites with selenium are reported, e.g., in the form of polymeric films as well as of polymers containing polyvinyl alcohol-stabilized selenium nanoparticles [33], polymer nanocomposites of selenium biofabricated using fungi [34], or composite materials for prosthetic dentures based on acrylic reinforced with nano-selenium [34]. In the study by Shah [33], it was found that the introduction of selenium nanoparticles caused a reduction in the mechanical properties (transverse, impact, and hardness) of an acrylic polymer, but the SeNPs were found to be an interesting material for anti-pollution processing (catalysis) and to design/control the physicochemical properties of polymer matrices.

This work aimed to use SeNPs as a catalyst and a filler of polymer matrices. For this purpose, SeNPs were firstly prepared and stabilized with starch and lignin derivatives. Second, SeNPs were used as a catalyst in the reduction process of a selected organic dye and as a filler for polymer matrices. The materials were tested mechanically (strength properties), thermally (thermal stability), and microscopically (surface morphology was examined to determine the dispersion of the filler). Our results provide new insights for the application of selenium nanoparticles.

2. Materials and Methods

2.1. Materials

Selenium (IV) oxide and ascorbic acid were received from Sigma Aldrich (Saint Louis, MO, USA), sodium lignosulfonate (LS) from softwood, molecular weight 6400 Da, was received from Borregaard LignoTech (Sarpsborg, Norway), and Sylobloc K500 silica was received from Grace GmbH & Co. (Columbia, MD, USA) KG. The monomers, 2-hydroxyethyl methacrylate (HEMA) and polyethylene glycol diacrylate, with MW = 575 (PEGDA), were purchased from Sigma Aldrich (Saint Louis, MO, USA) and were purified by column chromatography before use. The photoinitiator, 2,2-dimethoxy-2-phenylacetophenone (Irgacure 651) was also purchased from Sigma-Aldrich (Saint Louis, MO, USA).

2.2. Methods

2.2.1. Preparation of Sodium Starch Octenyl Succinate

Sodium starch octenyl succinate (OSA) containing 2.5% of octenyl succinate groups was synthesized according to the procedure described in [35].

2.2.2. Synthesis of SeNPs

The synthesis of colloidal selenium was carried out by chemical reduction using ascorbic acid as a reducer of the selenium compounds, selenium (IV) oxide and OSA, with LS as a stabilizers of the obtained SeNPs. The use of two different stabilizers made it possible to obtain selenium nanoparticles SeNPs in two forms, i.e., starch octenyl succinate provided selenium nanoparticles (SeNPs-OSA) on a solid matrix (=starch derivate), while the use of sodium lignosulfonate allowed obtaining SeNPs-LS in liquid form, which were used to impregnate the commercial silicon dioxide Sylobloc K500 in the next step.

A selenium solution with a concentration of 5.5 g/L was used for the study. Details about the preparation of the selenium nanoparticles: the concentration and the volume of SeO_2 were, respectively, 5.5 g/L and 40 mL, the concentration and the volume of the reducer $C_6H_8O_6$ were, respectively 42.2 g/L and 20 mL, the amount of the first stabilizer, sodium starch octenyl succinate (OSA), was 3 g, the concentration and the volume of the second stabilizer, a sodium salt of lignosulfonic acid (LS), were, respectively 18.75 g/L and 13.33 mL.

The resulting mixtures were stirred for 24 h at room temperature and then allowed to stand quiescent for a few days to complete the reaction. After this time, the resulting selenium nanoparticles were subjected to a physicochemical analysis. The obtained liquid selenium nanoparticles were also deposited on the commercial silica Sylobloc K500. The details of the prepared selenium nanoparticles are shown in Table 1.

2.2.3. Preparation of SeNPs–Matrix/Polymer

To obtain the SeNPs–carrier/polymer composite, a mixture of two monomers, i.e., 2-hydroxyethyl methacrylate (HEMA) and polyethyl glycol diacrylate (PEGDA) in a 2:3 ratio (by weight), was prepared. PEGDA was used as a crosslinking agent for the photopolymerization of HEMA in order to obtain HEMA/PEGDA-based polymers [36]. Following this preparation, the 2,2-dimethoxy-2-phenylacetophenone photoinitiator was added (1 wt% relative to the monomer mixture). SeNPs-OSA and SeNPs-LS842-Sylobloc K500 in the amounts of 1%, 3%, and 5% wt.% were added to mixture of the monomers. The homogenization process was carried out using a mechanical shaker (15 h, 3000 1/min) and

an ultrasonic bath (24 h, 50 kHz, 310 W). Samples of the polymer composite (dimensions: diameter 12 mm, thickness 1 mm) were obtained by the photopolymerization of the mixtures in a mold. The samples were irradiated for 3 min on both sides through PET foils with the full spectrum (320–395 nm) of a DYMAX-Blue Wave 50 lamp (Torrington, CT, USA).

Table 1. The details of the selenium nanoparticles.

Sample Name	Synthesis and Composition	
SeNPs-LS842 (liquid sample)	40 mL (5.5 g/L) SeO_2 20 mL (42.2 g/L) $C_6H_8O_6$—reducer 13.33 mL (18.75 g/L) sodium salt of lignosulfonic acid (LS)—liquid stabilizer	
SeNPs-OSA (solid sample)	40 mL (5.5 g/L) SeO_2 20 mL (42.2 g/L) $C_6H_8O_6$—reducer 3 g sodium starch octenyl succinate (OSA)—solid stabilizer	The components were stirred for 24 h at room temperature and then allowed to stand quiescent for a few days to complete the reaction.
SeNPs-LS842-Sylobloc K500 (solid sample)	40 mL (5.5 g/L) SeO_2 20 mL (42.2 g/L) $C_6H_8O_6$—reducer 13.33 mL (18.75 g/L) sodium salt of lignosulfonic acid (LS)—liquid stabilizer Commercial silica Sylobloc K500 used as a solid matrix	

2.2.4. SEM—Surface Composition and Imaging

A Scanning Electron Microscope (S-3400N, Hitachi, Tokyo, Japan) equipped with the EDS Ultradry Analysis Attachment (Thermo-Scientific, Waltham, MA, USA) was used. Based on energy-dispersion microanalysis, the selenium content was determined on individual matrices, and additionally, SEM micrographs of the solidified samples were acquired.

2.2.5. Catalytic Properties

The catalytic properties of the selenium colloids were checked using the USB 4000 UV–VIS spectrophotometer (Ocean Optics, Dunedin, FL, USA). In our study, methylene blue (C.I. Basic Blue 9) was used as a dye, and sodium borohydride ($NaBH_4$) was used as a reducer.

These properties were investigated for the SeNPs-LS842 colloidal system as well as for the SeNPs-OSA and SeNPs-LS842-Sylobloc K500 systems. The analysis was performed using methylene blue and sodium borohydride. In the case of a liquid sample—SeNPs-LS842 (see sample coding later on)—20 μL of selenium, 2 mL of the dye (4 mg/L), and 50 μL of sodium borohydride (10 g/L) were added to a measuring cuvette. Then. the absorption bands in the UV spectrum were recorded every 30 s. The study of nanoparticles in a solid form—SeNPs-OSA and SeNPs-LS842-Sylobloc K500—involved placing them in vials together with the dye and sodium borohydride (in an amount analogous to that of the liquid colloids) and then observing the color change of the organic dye.

2.2.6. Thermogravimetric Analysis

The thermogravimetric analysis (TGA) was performed using a PerkinElmer Pyris 1 TGA instrument (NETZSCH–Geratebau GmbH, Germany). The sample holder made of Pt was filled with approximately 10 mg of material. Mass loss measurements as a function of the temperature were performed from 25.0 to 590.0 °C, at a heating rate of 10.0 °C/min under a nitrogen atmosphere.

2.2.7. Mechanical Properties

The mechanical properties of the composite materials were studied at room temperature by testing the Young's modulus, tensile strength, elongation at break, and hardness according to PN-EN ISO 527-1:1998 (crosshead speed of 5 mm/min) with a Zwick/Roell universal testing machine, model Z020 (Zwick GmbH & Co. KG, Ulm, Germany). The

Shore A hardness was measured according to DIN 53 505. The results were averaged (at least 6 individual measurements for each sample).

2.2.8. Optical Microscopy

Optical microscopy images were collected using an Olympus BX60 microscope (Tokyo, Japan). The samples were fractured at room temperature.

2.2.9. Atomic Force Microscopy (AFM)

Following the optical microscopy analysis, the samples' surface was studied by AFM in air and at room temperature, using a MultiMode 8 instrument with a NanoScope V controller (Bruker, Billerica, MA, USA). The AFM was operated in the PeakForce Quantitative Nanomechanical Mapping mode (PF-QNM); thus, force–distance curves were recorded (512×512 per map) and further processed (NanoScope Analysis software, version 1.9). During scanning, the ScanAsyst control for the feedback loop gain and applied load was set to "off" to apply the chosen constant scanning parameters. The force–distance curves were collected following a sine-wave sample-tip trajectory with a frequency of 2 kHz and utilizing a peak-force amplitude value of 100–150 nm. Medium-soft cantilevers were chosen to conduct the imaging (nominal spring constant of 5 N/m, nominal radius of 10 nm, Budgetsensors, Tap150-G, Sofia, Bulgaria). The AFM optical sensitivity (deflection sensitivity) was calculated based on the thermal tune method [37].

3. Results and Discussion

In order to analyze and characterize the obtained biocomposites, i.e., the starch–selenium nanostructures (SeNPs-OSA) and the silica–lignosulfonate–selenium nanostructures (SeNPs-LS842-Sylobloc K500), tests of their surface structure and elemental composition (SEM, EDS, AFM analyses), stability (TGA), and selected mechanical properties, such as Young's modulus, tensile strength, elongation at break, and hardness, were carried out. The ability of the biocomposites to catalyze reduction reactions of selected dyes in model aqueous solutions was also studied.

3.1. Energy Dispersion Microanalysis (EDS) and SEM Imaging (Filler)

On the one hand, a significant amount of selenium (5.09%) was found by energy dispersion microanalysis (EDS) on the starch derivative (SeNPs-OSA, stabilizer OSA) (Figure 1). The EDS mapping of the sample area showed that the distribution of selenium on the surface of both starch and silica grains was uniform.

On the other hand, the impregnation of silicon dioxide with the selenium nanoparticles, where the stabilizer of the produced nanoparticles was a water-soluble lignin derivative (sodium lignosulfonate LS842), allowed for much smaller amounts of SeNPs (0.23%) on the solid matrix Sylobloc K500. Therefore, when the goal is to obtain solid selenium, it is much more advantageous to use the stabilizer in the correct form. The SEM micrographs indicated the shape and size of the obtained composites containing modified starch or silica and SeNPs. They showed small particles with diameters in the range of 10–50 μm for SeNPs-OSA and smaller particles for the SeNPs-LS842-Sylobloc K500 systems, with a diameter below 5 μm (Figure 2). Selenium nanoparticles were deposited on the surface of starch or silica grains (which was confirmed by the EDS analysis). The recorded starch grain size was characteristic of potato starch grains. Visible damage to the middle part of the grain (cup-shaped grain) was caused by the chemical modification of the native starch.

3.2. Selenium as a Catalyst for Reduction Reactions

In chemistry, one of the strongest and most effective reducing agents is sodium borohydride, but many reduction reactions are kinetically inhibited. These kinds of reactions require a longer time to be completed or a larger amount of a reducer. However, sodium borohydride has low stability and auto-decomposes in aqueous media. The problem can

be solved by introducing nanostructures of elements such as gold, silver, or selenium into the system [26].
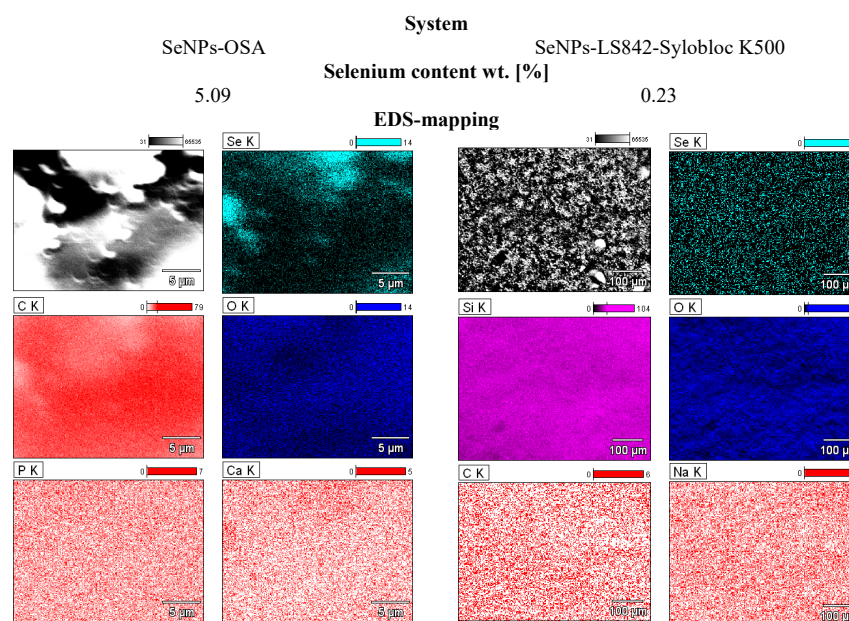

Figure 1. Selenium content in individual matrices—EDS analysis.
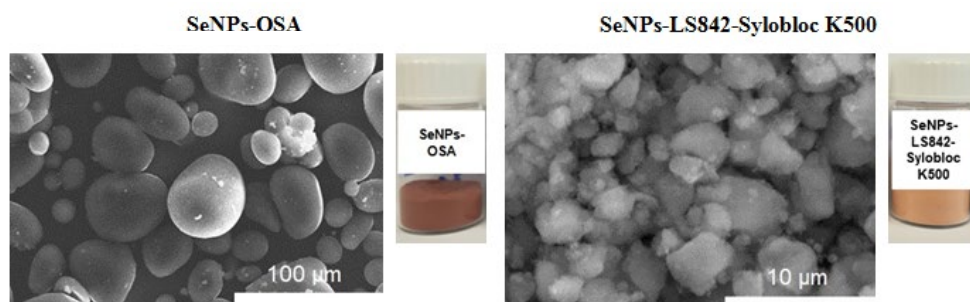

Figure 2. Selenium content in individual matrices—SEM pictures and photographs of the obtained samples.

The measured UV–Vis absorbance spectra of the colloid in liquid form (SeNPs-LS842) confirmed the catalytic ability of the produced selenium nanoparticles (Figure 3).

After adding the selenium colloid to the dye and reducing agent mixture ($NaBH_4$), a gradual decrease in the UV–Vis absorbance in the dye spectrum was observed. This proves the catalytic ability of the nanostructures used. During the first 3 min from the initiation of the reduction process, the spectrum of methylene blue rapidly decreased, so that, after approx. 25 min, the entire dye was reduced. The catalytic efficiency of SeNPs in solid form, i.e., SeNPs-OSA and the SeNPs-LS842-Sylobloc K500 systems, was also studied (Figure 4).

In the vial containing the organic dye and sodium borohydride (Figure 4A), no color change was observed for a long time. However, the systems enriched with SeNPs on a starch derivative—SeNPs-OSA (Figure 4B)—or silica—SeNPs-LS842-Sylobloc K500 (Figure 4C)—discolored; hence, one can conclude that the SeNPs also catalyzed the dye reduction reaction.

3.3. Thermogravimetric Analysis

A thermogravimetric analysis of the obtained copolymers filled with SeNPs-OSA or SeNPs-LS842-Sylobloc K500 was performed (Figure 5). This analysis confirmed the stability of the obtained copolymers and composites. At temperatures below 140 °C, the weight loss for all samples was similar. at around 3%. In the higher temperature range, 140–330 °C, the

weight loss was still negligible and oscillated around 5%. It was only above 330 °C that thermal decomposition of the samples occurred. The mass of the dry residue corresponded to the filler content in the composite material.
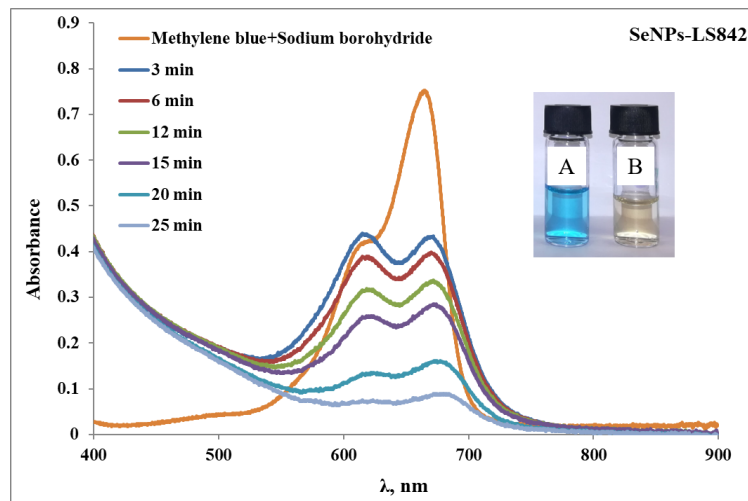

Figure 3. UV–Vis absorbance spectra for SeNPs in liquid form; inset photos: A—methylene blue and sodium borohydride, B—methylene blue, sodium borohydride, and SeNPs-LS842 25 min after the addition of the selenium nanoparticles.
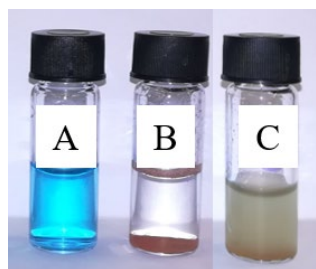

Figure 4. Catalytic properties of SeNPs. (**A**)—methylene blue and sodium borohydride, (**B**)—methylene blue, sodium borohydride, and SeNPs-OSA 90 s after the addition of the selenium nanoparticles, (**C**)—methylene blue, sodium borohydride, and SeNPs-LS842-Sylobloc K500 6 min after the addition selenium nanoparticles.
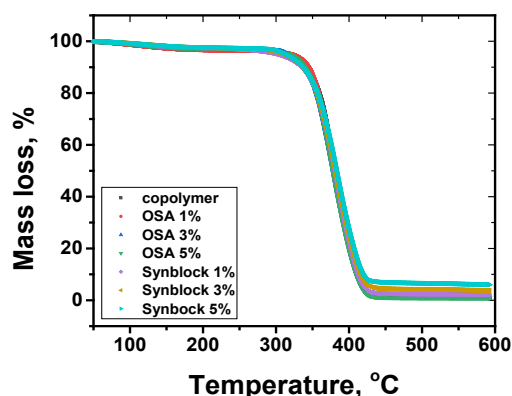

Figure 5. Thermogravimetric curves of the neat copolymer filled with SeNPs-OSA or SeNPs-LS842-Sylobloc K500 at the indicated contents.

3.4. Influence of the SeNPs–Carrier System on the Mechanical Parameters of the Composite Materials

The applications of polymers are always limited due to their poor mechanical properties. The mechanical properties of a polymer composite are affected by the filler used, as well as by the continuous phase.

The studied composite polymers varied in strength properties depending on their composition, as well as on the filler content (Figure 6). Depending on the selenium content and the filler type, various correlations were noted. The Young's modulus increased with an increase in the filler content, indicating an increase in the material stiffness caused by the fact that chain mobility and intermolecular motion became more difficult in the composite, and the added inorganic particles had a higher stiffness than the polymer matrices (Figure 6a). With a 5% content of the SeNPs-LS842-Sylobloc K500 filler, the Young's modulus value increased by 57% compared to the Young's modulus obtained for the unfilled copolymer. Since the Young's modulus of a polymer composite depend on the properties of its ingredients (matrix and filler) and only to a slight extent on their interfacial adhesion, both types of fillers contribute to the modulus increase in a similar way. However, the strength strongly depends on the stress transfer between particles and the polymer matrix. When there is a good interaction between the matrix and the particles, the applied stresses can be effectively transferred to the particles from the matrix, thus enhancing the strength. As in the case of the Young's modulus, the strength of the composite materials containing SeNPs-LS842-Sylobloc K500 also increased with the increasing filler content (Figure 6b). In contrast to the Young's modulus, the tensile strength is very sensitive to interfacial adhesion and can therefore be used even as an indicator of the copolymer/filler interactions. The filler with SeNPs-OSA (Figure 6b) did not ensure such large interactions between the filler and the polymer matrix, and as a result, it did not affect the strength properties of the obtained composite materials effectively; in addition, agglomerates of large sizes were responsible for creating an additional stress concentration that facilitated the samples' cracking.
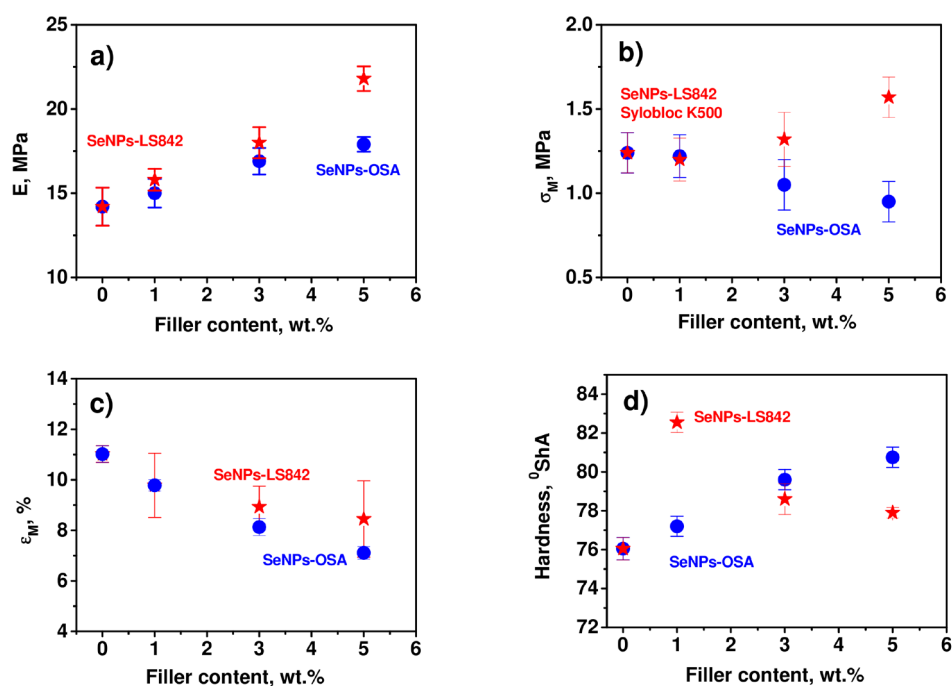

Figure 6. Young's modulus E (**a**), tensile strength δ_M (**b**), elongation at break ε_M (**c**), and hardness (**d**) as a function of the filler content.

According to the literature data, the value of elongation at break usually decreases after adding the filler, which was also visible in our case [38]. The introduction of an inorganic

filler strengthened the polymer matrix at the expense of deteriorating its plasticity, which resulted in a decrease in the value of ε_M (Figure 6c). Elongation at break reflects the ductility of an investigated sample. A decrease in ductility occurred and indicated a reduction in the matrix deformation due to the mechanical restraints imposed by the almost non-deformable filler particles, which made the material more brittle and relatively weak.

The hardness of both types of composites increased with the filler content (Figure 6d). This resulted from the increased moduli and the presence of hard filler domains. Somewhat surprising was the hardness of the SeNPs-LS842-Sylobloc K500-filled materials, although this parameter was expected to be higher for this filler. One can speculate that this resulted from the lower crosslinking density of SeNPs-LS842-Sylobloc K500 with the polymer matrix.

3.5. AFM and Optical Microscopy Analysis of the Composites

The optical microscopy images (Figure 7) of the fractured copolymer and its composites showed typical cracking features (crack propagation) across the bulk surface. As the SeNPs-LS842-Sylobloc K500 sample employed the smallest—in terms of size—filler, the sample surface showed many crack propagation lines, but with a modest bulk penetration (white arrows). Since a crack typically starts and ends at the fillers, one can appreciate the good filler dispersity in the matrix in the images shown. Locally, the copolymer sample surface was flat enough for AFM imaging to be performed. The surface of the copolymer was found to be homogeneous, with a room mean square roughness of only 8.3 nm. The (surface) deformation and adhesion force maps showed a slight change in value (see cross-section plots) that indicated a good mixability of the monomers used in the study (monophase surface morphology). Due to the size of the fillers used, AFM imaging of the composites was not possible within the AFM scanner range.
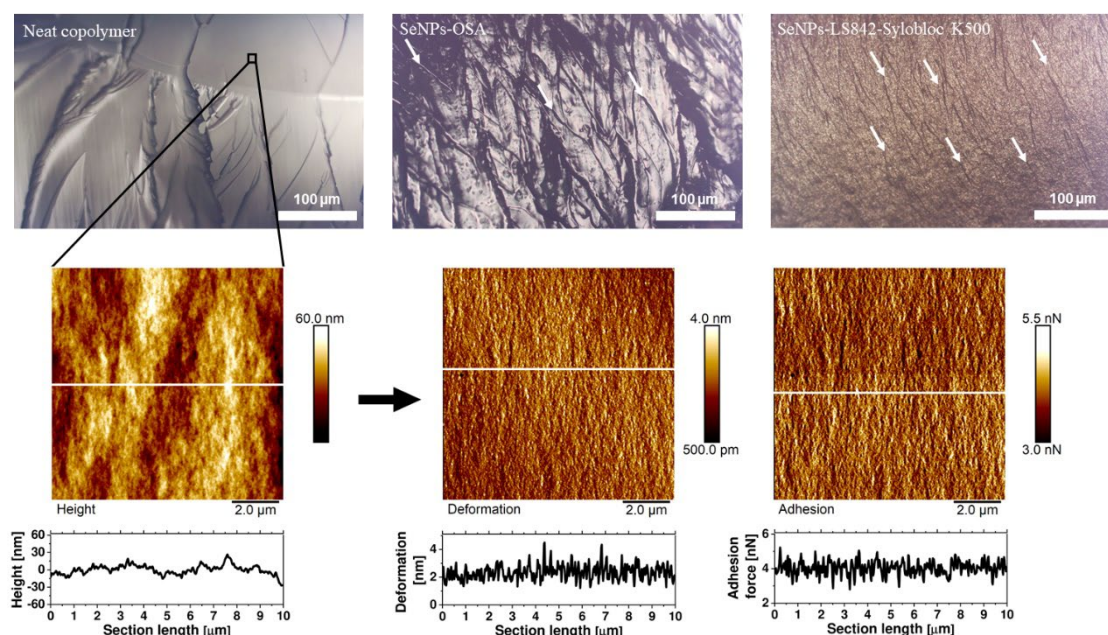

Figure 7. Optical microscopy of the neat copolymer and of the copolymer filled with SeNPs–OSA or SeNPs–LS842–Sylobloc K500 at the highest content (5% wt.) White arrows indicate examples of crack propagation and their directions. AFM images with the cross-section plots represent the height, deformation, and adhesion force mapping of the area indicated by the black square.

To sum up, the filler SeNPs-LS842-Sylobloc K500 turned out to be the most optimal additive. Even its small admixture (1% by weight) improved the stiffness and hardness of the copolymer material.

4. Conclusions

Selenium nanoparticles, both in liquid form (SeNPs-LS842) and in combination with a suitable matrix (SeNPs-OSA or SeNPs-LS842-Sylobloc K500), have catalytic properties that can be used in the reduction of organic dyes. Furthermore, natural biopolymers, such as sodium lignosulfonate and starch octenyl succinate, can be used as stabilizers for the obtained nanoparticles.

In this article, the process and properties of methacrylate and acrylate-based compounds containing SeNPs-OSA were investigated and compared with those of compounds containing SeNPs-LS842-Sylobloc K500. As a result, it can be stated that tensile strength and elongation at break of the SeNPs-LS842-Sylobloc K500-filled materials increased monotonically within the whole range of the filler content, but elongation at break of the SeNPs-OSA filled materials decreased due to mechanical restraints imposed by the almost non-deformable filler, which made the material more brittle. Furthermore, studies have shown that even a small admixture of SeNPs-LS842-Sylobloc K500 significantly improved the stiffness and hardness of polymer materials. Last but not least, the copolymers obtained appeared to be thermostable at a temperature below 330 °C.

Author Contributions: Conceptualization, A.M.-S., M.R. and E.K.; methodology, A.M.-S., M.R. and E.K.; software, M.R. and Ł.G.; validation, A.M.-S., M.R. and Ł.G.; formal analysis, A.M.-S., M.R. and H.G.; investigation, A.M.-S., M.R., E.K. and H.G.; resources, A.M.-S., M.R. and E.K.; data curation, A.M.-S. and M.R.; writing—original draft preparation, A.M.-S., M.R., E.K., H.G. and Ł.G.; writing—review and editing, A.M.-S., M.R., H.G., Ł.G., B.W., Ł.W. and W.Ł.; visualization, A.M.-S., M.R. and Ł.G.; supervision, A.M.-S. and Ł.G.; project administration, A.M.-S. and M.R.; funding acquisition, Ł.G. All authors have read and agreed to the published version of the manuscript.

Institutional Review Board Statement: Not applicable.

Informed Consent Statement: Not applicable.

Data Availability Statement: Not applicable.

Conflicts of Interest: The authors declare no conflict of interest.

References

1.　Presentato, A.; Piacenza, E.; Anikovskiy, M.; Cappelletti, M.; Zannoni, D.; Turner, R.J. Biosynthesis of selenium-nanoparticles and -nanorods as a product of selenite bioconversion by the aerobic bacterium *Rhodococcus aetherivorans* BCP1. *New Biotechnol.* **2018**, *41*, 1–8. [CrossRef]

2.　Diko, C.S.; Zhang, H.; Lian, S.; Fan, S.; Li, Z.; Qu, Y. Optimal synthesis conditions and characterization of selenium nanoparticles in *Trichoderma* sp. WL-Go culture broth. *Mater. Chem. Phys.* **2020**, *246*, 122583. [CrossRef]

3.　Vahdati, M.; Moghadam, T.T. Synthesis and Characterization of Selenium Nanoparticles-Lysozyme Nanohybrid System with Synergistic Antibacterial Properties. *Sci. Rep.* **2020**, *10*, 510. [CrossRef] [PubMed]

4.　Tripathi, R.M.; Hameed, P.; Rao, R.P.; Shrivastava, N.; Mittal, J.; Mohapatra, S. Biosynthesis of Highly Stable Fluorescent Selenium Nanoparticles and the Evaluation of Their Photocatalytic Degradation of Dye. *Bionanoscience* **2020**, *10*, 389–396. [CrossRef]

5.　Jamróz, E.; Kulawik, P.; Kopel, P.; Balková, R.; Hynek, D.; Bytesnikova, Z.; Gagic, M.; Milosavljevic, V.; Adam, V. Intelligent and active composite films based on furcellaran: Structural characterization, antioxidant and antimicrobial activities. *Food Packag. Shelf Life* **2019**, *22*, 100405. [CrossRef]

6.　Menon, S.; Ks, S.D.; Santhiya, R.; Rajeshkumar, S.; Kumar, V. Selenium nanoparticles: A potent chemotherapeutic agent and an elucidation of its mechanism. *Colloids Surf. B Biointerfaces* **2018**, *170*, 280–292. [CrossRef]

7.　Umar, A.; Khan, M.S.; Alam, S.; Zekker, I.; Burlakovs, J.; Rubin, S.S.; Bhowmick, G.D.; Kallistova, A.; Pimenov, N.; Zahoor, M. Synthesis and Characterization of Pd-Ni Bimetallic Nanoparticles as Efficient Adsorbent for the Removal of Acid Orange 8 Present in Wastewater. *Water* **2021**, *13*, 1095. [CrossRef]

8.　Lai, S.K.M.; Tang, H.-W.; Lau, K.C.; Ng, K.M. Nanosecond UV Laser Ablation of Gold Nanoparticles: Enhancement of Ion Desorption by Thermal-Driven Desorption, Vaporization, or Phase Explosion. *J. Phys. Chem. C* **2016**, *120*, 20368–20377. [CrossRef]

9.　Panahi-Kalamuei, M.; Salavati-Niasari, M.; Zarghami, Z.; Mousavi-Kamazani, M.; Taqriri, H.; Mohsenikia, A. Synthesis and characterization of Se nanostructures via co-precipitation, hydrothermal, microwave and sonochemical routes using novel starting reagents for solar cells. *J. Mater. Sci. Mater. Electron.* **2015**, *26*, 2851–2860. [CrossRef]

10. Qiao, L.; Dou, X.; Yan, S.; Zhang, B.; Xu, C. Biogenic selenium nanoparticles synthesized by *Lactobacillus casei* ATCC 393 alleviate diquat-induced intestinal barrier dysfunction in C57BL/6 mice through their antioxidant activity. *Food Funct.* **2020**, *11*, 3020–3031. [CrossRef]

11. Mates, I.; Antoniac, I.; Laslo, V.; Vicas, S.; Brocks, M.; Luminita, F.; Milea, C.; Mohan, A.; Cavalu, S. Selenium nanoparticles: Production, characterization and possible applications in biomedicine and food science. *Sci. Bull. B Chem. Mater. Sci. UPB* **2019**, *81*, 205–216.

12. Alam, H.; Khatoon, N.; Raza, M.; Ghosh, P.C.; Sardar, M. Synthesis and Characterization of Nano Selenium Using Plant Biomolecules and Their Potential Applications. *BioNanoScience* **2019**, *9*, 96–104. [CrossRef]

13. Sohouli, E.; Irannejad, N.; Ziarati, A.; Ehrlich, H.; Rahimi-Nasrabadi, M.; Ahmadi, F.; Luque, R. Application of polysaccharide-based biopolymers as supports in photocatalytic treatment of water and wastewater: A review. *Environ. Chem. Lett.* **2022**, *20*, 3789–3809. [CrossRef]

14. Mukherjee, S.; Mukhopadhyay, S. Recent progress in sulfur-containing technical lignin-based polymer composites. *Express Polym. Lett.* **2023**, *17*, 120–151. [CrossRef]

15. Ndwandwe, B.K.; Malinga, S.P.; Kayitesi, E.; Dlamini, B.C. Selenium nanoparticles–Enhanced potato starch film for active food packaging application. *Int. J. Food Sci. Technol.* **2022**, *57*, 6512–6521. [CrossRef]

16. Modrzejewska-Sikorska, A.; Konował, E.; Klapiszewski, Ł.; Nowaczyk, G.; Jurga, S.; Jesionowski, T.; Milczarek, G. Lignosulfonate-stabilized selenium nanoparticles and their deposition on spherical silica. *Int. J. Biol. Macromol.* **2017**, *103*, 403–408. [CrossRef]

17. Hu, T.Q. *Chemical Modification, Properties, and Usage of Lignin*; Springer: New York, NY, USA, 2002.

18. Belgacem, A.G.M.N. *Monomers, Polymers and Composites from Renewable Resources*, 1st ed.; Elsevier: Amsterdam, The Netherlands, 2008.

19. Qiu, X.; Kong, Q.; Zhou, M.; Yang, D. Aggregation behavior of sodium lignosulfonate in water solution. *J. Phys. Chem. B* **2010**, *114*, 15857–15861. [CrossRef] [PubMed]

20. Vishtal, A.; Kraslawski, A. Challenges in industrial applications of technical lignins. *BioResources* **2011**, *6*, 3547–3568. [CrossRef]

21. Vanholme, R.; Morreel, K.; Ralph, J.; Boerjan, W. Lignin engineering. *Curr. Opin. Plant Biol.* **2008**, *11*, 278–285. [CrossRef] [PubMed]

22. Pang, Y.X.; Qiu, X.Q.; Yang, D.J.; Lou, H.M. Influence of oxidation, hydroxymethylation and sulfomethylation on the physico-chemical properties of calcium lignosulfonate. *Colloids Surf. A Physicochem. Eng. Asp.* **2008**, *312*, 154–159. [CrossRef]

23. Yan, M.; Yang, D.; Deng, Y.; Chen, P.; Zhou, H.; Qiu, X. Influence of pH on the behavior of lignosulfonate macromolecules in aqueous solution. *Colloids Surf. A Physicochem. Eng. Asp.* **2010**, *371*, 50–58. [CrossRef]

24. Deng, Y.; Wu, Y.; Qian, Y.; Ouyang, X.; Yang, D.; Qiu, X. Adsorption and desorption behaviors of lignosulfonate during the self-assembly of multilayers. *BioResources* **2010**, *2010*, 1178–1196.

25. Konował, E.; Modrzejewska-Sikorska, A.; Milczarek, G. Synthesis and multifunctional properties of lignosulfonate-stabilized gold nanoparticles. *Mater. Lett.* **2015**, *159*, 451–454. [CrossRef]

26. Modrzejewska-Sikorska, A.; Konował, E.; Cichy, A.; Nowicki, M.; Jesionowski, T.; Milczarek, G. The effect of silver salts and lignosulfonates in the synthesis of lignosulfonate-stabilized silver nanoparticles. *J. Mol. Liq.* **2017**, *240*, 80–86. [CrossRef]

27. Modrzejewska-Sikorska, A.; Konował, E. Silver and gold nanoparticles as chemical probes of the presence of heavy metal ions. *J. Mol. Liq.* **2020**, *302*, 112559. [CrossRef]

28. Sweedman, M.C.; Tizzotti, M.J.; Schäfer, C.; Gilbert, R.G. Structure and physicochemical properties of octenyl succinic anhydride modified starches: A review. *Carbohydr. Polym.* **2013**, *92*, 905–920. [CrossRef]

29. Caldwell, C.G.; Wurzburg, O.B. Polysaccharide Derivatives of Substituted Dicarboxylic Acids. U.S. Patent 2,661,349, 1 December 1953.

30. Khatami, M.; Iravani, S. Green and Eco-Friendly Synthesis of Nanophotocatalysts: An Overview. *Comments Inorg. Chem.* **2021**, *41*, 133–187. [CrossRef]

31. Nguyen, N.T.T.; Nguyen, L.M.; Nguyen, T.T.T.; Liew, R.K.; Nguyen, D.T.C.; van Tran, T. Recent advances on botanical biosynthesis of nanoparticles for catalytic, water treatment and agricultural applications: A review. *Sci. Total Environ.* **2022**, *827*, 154160. [CrossRef]

32. Asl, F.D.; Mousazadeh, M.; Azimzadeh, M.; Ghaani, M. Mesoporous selenium nanoparticles for therapeutic goals: A review. *J. Nanoparticle Res.* **2022**, *24*, 210. [CrossRef]

33. Shah, C.P.; Singh, K.K.; Kumar, M.; Bajaj, P.N. Vinyl monomers-induced synthesis of polyvinyl alcohol-stabilized selenium nanoparticles. *Mater. Res. Bull.* **2010**, *45*, 56–62. [CrossRef]

34. Tsivileva, O.; Pozdnyakov, A.; Ivanova, A. Polymer Nanocomposites of Selenium Biofabricated Using Fungi. *Molecules* **2021**, *26*, 3657. [CrossRef] [PubMed]

35. Prochaska, K.; Kędziora, P.; Le Thanh, J.; Lewandowicz, G. Surface properties of enzymatic hydrolysis products of octenylsuccinate starch derivatives. *Food Hydrocoll.* **2007**, *21*, 654–659. [CrossRef]

36. González-Henríquez, C.M.; Del Pizarro, G.C.; Sarabia-Vallejos, M.A.; Terraza, C.A.; López-Cabaña, Z.E. In situ-preparation and characterization of silver-HEMA/PEGDA hydrogel matrix nanocomposites: Silver inclusion studies into hydrogel matrix. *Arab. J. Chem.* **2019**, *12*, 1413–1423. [CrossRef]

37. Hutter, J.L.; Bechhoefer, J. Calibration of atomic-force microscope tips. *Rev. Sci. Instrum.* **1993**, *64*, 1868–1873. [CrossRef]
38. Aso, O.; Eguiazábal, J.I.; Nazábal, J. The influence of surface modification on the structure and properties of a nanosilica filled thermoplastic elastomer. *Compos. Sci. Technol.* **2007**, *67*, 2854–2863. [CrossRef]